

A METHOD OF ANALYSIS FOR HORIZONTALLY EMBEDDED ANCHORS IN AN ELASTIC SOIL

R. K. ROWE AND J. R. BOOKER

Department of Civil Engineering, The University of Sydney, Sydney, Australia

SUMMARY

A general method is presented for the analysis of horizontally embedded anchors in an elastic soil. Provision is made in the analysis for the consideration of anchor shape, layer depth, anchor-soil interface condition, breakaway of the anchor from the underlying soil and interaction between groups of anchors.

Application of the analytical technique is illustrated for strip and circular anchors, and these solutions are presented in the form of influence charts which may be used directly in hand calculations to predict the elastic load deflection behaviour of anchor plates for a wide variety of material and geometric conditions.

INTRODUCTION

Although the behaviour of anchor plates at working loads is of considerable practical importance, previous investigations into the elastic load-deflection behaviour of horizontal anchors have been restricted to the case of a fully bonded, perfectly flexible or infinitely rigid anchor resting in either an elastic half-space (Fox¹) or within an infinite elastic mass (Selvadurai²). In this paper, an analytical technique will be presented for the analysis of an anchor of general shape buried at a depth h below the surface of an isotropic elastic soil layer (with elastic modulus E and Poisson's ratio ν) which extends a further distance D below the anchor plate. The anchor plate itself may be either perfectly flexible or rigid while the anchor-soil interface may be either smooth or rough. In addition, provision is made for slip between anchor and soil as well as breakaway of the anchor from the underlying soil.

THEORY

Development of the solution method

Referring to Figure 1, R is a horizontal anchor plate embedded in an elastic layer. The horizontal plane containing the anchor R ($z = z_0$) divides the layer into two parts $\Gamma^{(+)}$ ($z_0 < z < z^{(+)}$) above the anchor and $\Gamma^{(-)}$ ($z^{(-)} < z < z_0$) below the anchor. The stress and displacement fields in $\Gamma^{(+)}$, $\Gamma^{(-)}$ will be denoted by the superscripts (+), (-), respectively. In general, these quantities will suffer a 'dislocation' at the interface R owing to the presence of the plate. Thus, for example, the vertical stress just above and just below the plate will in general differ, owing to the action of the applied load on the plate, and the horizontal displacements above and below the plate may differ owing to slip at the soil-plate interface.

In the most general case, the quantity

$$\mathbf{p}^T = (\sigma_{zx}, \sigma_{zy}, \sigma_{zz}, u, v, w) \quad (1a)$$

R. K. ROWE AND J. R. BOOKER

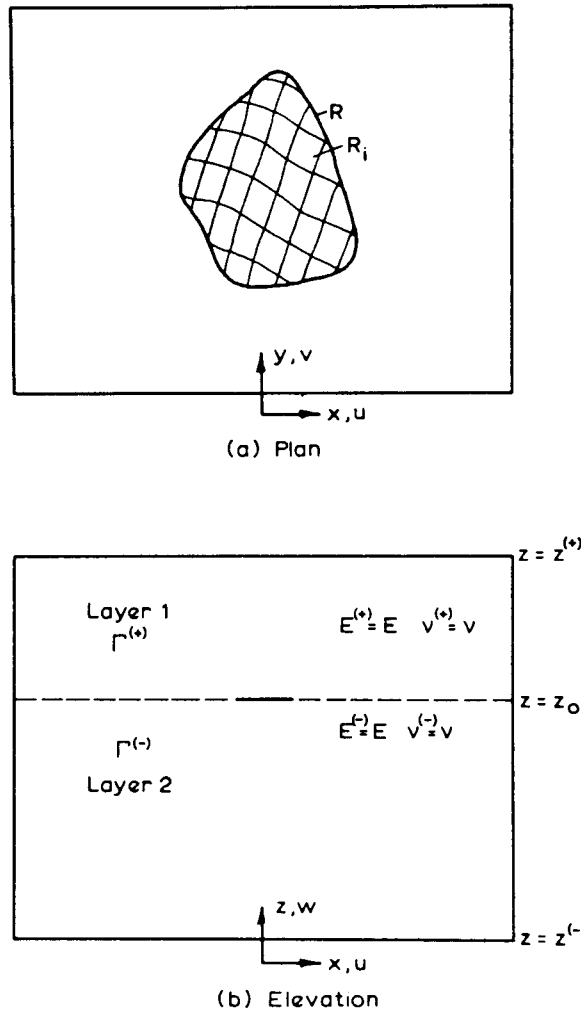


Figure 1. Analytical configuration

will undergo the jump

$$\Delta \mathbf{p} = \mathbf{p}^{(+)} - \mathbf{p}^{(-)} \quad (1b)$$

at the interface.

In order to analyse the behaviour of the anchor plate, suppose that the region R is divided into n sub-regions R_i as indicated in Figure 1. Further suppose that, to sufficient accuracy, it can be assumed that $\Delta \mathbf{p}$ takes the constant value $\Delta \mathbf{p}_i$ over each sub-region R_i .

In the following section, it will be shown how it is possible to express the field quantity $\mathbf{q}^T = (\sigma_{zx}^{(-)}, \sigma_{zy}^{(-)}, \sigma_{zz}^{(-)}, u^{(+)}, v^{(+)}, w^{(+)})$ on the plane $z = z_0$ in terms of the value $\Delta \mathbf{p}_i$ and in particular, that it is possible to establish the relation

$$\bar{\mathbf{q}}_j = \sum_{k=1}^n I_{jk} \mathbf{p}_k \quad (2)$$

HORIZONTALLY EMBEDDED ANCHORS

where I_{jk} is a 6×6 matrix of influence coefficients and

$$\bar{q}_j = \frac{1}{A_j} \int_{R_j} q \, dA$$

is the average value of q over the region R_j .

Equation (2) may be rewritten in the partitioned matrix form:

$$\begin{bmatrix} \mathbf{q}_1 \\ \vdots \\ \mathbf{q}_n \end{bmatrix} = \begin{bmatrix} I_{11} & \dots & I_{1n} \\ \vdots & \ddots & \vdots \\ I_{n1} & \dots & I_{nn} \end{bmatrix} \cdot \begin{bmatrix} \Delta \mathbf{p}_1 \\ \vdots \\ \Delta \mathbf{p}_n \end{bmatrix} \quad (3)$$

The above relation represents a set of $6n$ equations connecting the $6n$ average quantities $(\bar{\sigma}_{xx}^{(-)}, \bar{\sigma}_{zy}^{(-)}, \bar{\sigma}_{zz}^{(-)}, \bar{u}^{(+)}, \bar{v}^{(+)}, \bar{w}^{(+)})_i$, and the $6n$ quantities $(\Delta \sigma_{xx}, \Delta \sigma_{zy}, \Delta \sigma_{zz}, \Delta u, \Delta v, \Delta w)_i$.

This relationship can be used to solve a variety of problems by specifying the appropriate stress, displacement and dislocation conditions at the interface. In particular, provision can be made for either a rough or smooth anchor with or without breakaway of the anchor from the underlying region in $\Gamma^{(-)}$. For example, consider a smooth anchor subjected to a prescribed vertical displacement w_0 . Provided it is assumed that the anchor-soil interface cannot sustain tensile tractions, then breakaway of the anchor from the underlying region in $\Gamma^{(-)}(z = z_0)$ will occur over the sub-region R_i if, and only if, the normal traction acting on that portion of the interface has reached zero. Consequently, the general case where there is progressive breakaway with increasing load can be analysed by following an incremental procedure in which breakaway occurs over a sub-region R_i when the vertical stress at the interface of R_i with $\Gamma^{(-)}(z = z_0)$ reaches zero. Prior to breakaway the quantities $(w^{(+)}, \sigma_{xx}^{(-)}, \sigma_{zy}^{(-)}, \Delta w, \Delta \sigma_{xx}, \Delta \sigma_{zy})_i$ take the specified values $(w_0, 0, 0, 0, 0, 0)$ whereas after breakaway the 6 quantities $(w^{(+)}, \sigma_{xx}^{(-)}, \sigma_{zy}^{(-)}, \sigma_{zz}^{(-)}, \Delta \sigma_{xx}, \Delta \sigma_{zz})_i$ take the specified values $(w_0, 0, 0, 0, 0, 0)$. Equation (3) then represents a set of $6n$ equations in $6n$ unknowns for each increment of load

Determination of influence coefficients

In order to determine the influence coefficients of equations (2) and (3), the equations of elasticity are transformed by the application of a double Fourier transform (Sneddon³), or equivalently the field quantities are assumed to have a Fourier representation. Thus, typically, the displacement in the x direction will have the representation:

$$u(x, y, z) = \int_{-\infty}^{\infty} \int_{-\infty}^{\infty} e^{+i(\alpha x + \beta y)} U(\alpha, \beta, z) \, d\alpha \, d\beta \quad (4a)$$

where

$$U(\alpha, \beta, z) = \frac{1}{4\pi^2} \int_{-\infty}^{\infty} \int_{-\infty}^{\infty} e^{-i(\alpha x + \beta y)} u(x, y, z) \, dx \, dy \quad (4b)$$

In order to be specific in what follows, it will be assumed that the anchor plate is embedded in a single layer of a homogeneous elastic material, although the technique has a much more general application and may be extended to allow consideration of layered cross-anisotropic deposits (e.g., Gerrard⁴ and Gerrard and Harrison⁵).

Introduction of the Fourier representation, equation (4a), enables the solution in the upper portion of the layer (Γ^{+}) to be expressed in the form

$$\mathbf{P}^{(+)} = M(\alpha, \beta, z) \cdot \mathbf{c}^{(+)} \quad (5a)$$

where

$$\mathbf{P}^{(+)} = (\Sigma_{zx}, \Sigma_{zy}, \Sigma_{zz}, U, V, W)^T$$

is the vector of transforms of

$$(\sigma_{zx}, \sigma_{zy}, \sigma_{zz}, u, v, w)^T$$

$\mathbf{c}^{(+)}$ is a vector of 6 arbitrary constants

and

$M(\alpha, \beta, z)$ is the matrix defined in Table I.

Similarly, the solution in the lower portion of the layer (Γ^-) may be represented in the form

$$\mathbf{P}^{(-)} = M(\alpha, \beta, z)\mathbf{c}^{(-)} \quad (5b)$$

The 12 constants $\mathbf{c}^{(+)}$, $\mathbf{c}^{(-)}$ may be determined from the 3 boundary conditions at the upper surface ($z = z^{(+)}$), the 3 boundary conditions at the lower surface ($z = z^{(-)}$) and the 6 'jump' conditions at the interface ($z = z_0$), by solving

$$A \cdot \mathbf{c} = \mathbf{b} \quad (6)$$

where

$$\mathbf{c} = \begin{bmatrix} \mathbf{c}^{(+)} \\ \mathbf{c}^{(-)} \end{bmatrix}$$

and where A and \mathbf{b} are given in Table II, for the specific case of an elastic layer resting on a rough rigid base and with a stress free upper surface.

The solution of equation (5) leads to the relations

$$\mathbf{c}^{(+)} = N^{(+)}(\alpha, \beta) \cdot \Delta \mathbf{P} \quad (7a)$$

$$\mathbf{c}^{(-)} = N^{(-)}(\alpha, \beta) \cdot \Delta \mathbf{P} \quad (7b)$$

where it will be recognized that the 6×6 matrices $N^{(+)}(\alpha, \beta)$ and $N^{(-)}(\alpha, \beta)$ can be obtained by deleting columns 1-3 and 10-12 from A^{-1} , and then deleting rows (7-12) and (1-6), respectively.

It now follows from equations (5a) and (7a) and equations (5b) and (7b) that

$$\mathbf{P}^{(+)} = M(\alpha, \beta, z) \cdot N^{(+)}(\alpha, \beta) \cdot \Delta \mathbf{P}$$

and

$$\mathbf{P}^{(-)} = M(\alpha, \beta, z) \cdot N^{(-)}(\alpha, \beta) \cdot \Delta \mathbf{P}$$

and hence

$$\mathbf{Q} = (D^{(-)} \cdot M(\alpha, \beta, z_0) \cdot N^{(-)}(\alpha, \beta) + D^{(+)} M(\alpha, \beta, z_0) \cdot N^{(+)}(\alpha, \beta)) \cdot \Delta \mathbf{P} \quad (8)$$

where $D^{(-)}$ and $D^{(+)}$ are (6×6) matrices with zero components except for values of unity corresponding to the first three and last three diagonal terms, respectively.

It follows from the representation formulae, such as equation (4a), that

$$\mathbf{q} = \int_{-\infty}^{\infty} \int_{-\infty}^{\infty} e^{i(\alpha x + \beta y)} (D^{(-)} M(\alpha, \beta, z_0) N^{(-)}(\alpha, \beta) + D^{(+)} \cdot M(\alpha, \beta, z_0) \cdot N^{(+)}(\alpha, \beta)) \cdot \Delta \mathbf{P} \, d\alpha \, d\beta \quad (9)$$

Table I

$[M(\alpha, \beta, z)] =$	$M_{11}(z) = \left[\frac{i\alpha}{\gamma} - 2i\alpha\theta z \right] G e^{\gamma z}$	$M_{12}(z) = - \left[\frac{i\alpha}{\gamma} + 2i\alpha\theta z \right] G e^{-\gamma z}$	$M_{13}(z) = 2i\alpha\gamma G e^{\gamma z}$	$M_{14}(z) = -2i\alpha\gamma G e^{-\gamma z}$	$M_{15}(z) = \beta\gamma G e^{\gamma z}$	$M_{16}(z) = -\beta\gamma G e^{-\gamma z}$
	$M_{21}(z) = \left[\frac{i\beta}{\gamma} - 2i\beta\theta z \right] G e^{\gamma z}$	$M_{22}(z) = - \left[\frac{i\beta}{\gamma} + 2i\beta\theta z \right] G e^{-\gamma z}$	$M_{23}(z) = 2i\beta\gamma G e^{\gamma z}$	$M_{24}(z) = -2i\beta\gamma G e^{-\gamma z}$	$M_{25}(z) = -\alpha\gamma G e^{\gamma z}$	$M_{26}(z) = \alpha\gamma G e^{-\gamma z}$
	$M_{31}(z) = [\lambda + 2G(1 - \gamma\theta z)] e^{\gamma z}$	$M_{32}(z) = [\lambda + 2G(1 + \gamma\theta z)] e^{-\gamma z}$	$M_{33}(z) = 2G\gamma^2 e^{\gamma z}$	$M_{34}(z) = 2G\gamma^2 e^{-\gamma z}$	$M_{35}(z) = 0$	$M_{36}(z) = 0$
	$M_{41}(z) = -\frac{i\alpha\theta}{\gamma} z e^{\gamma z}$	$M_{42}(z) = \frac{i\alpha\theta}{\gamma} z e^{-\gamma z}$	$M_{43}(z) = i\alpha e^{\gamma z}$	$M_{44}(z) = i\alpha e^{-\gamma z}$	$M_{45}(z) = \beta e^{\gamma z}$	$M_{46}(z) = \beta e^{-\gamma z}$
	$M_{51}(z) = -\frac{i\beta\theta}{\gamma} z e^{\gamma z}$	$M_{52}(z) = \frac{i\beta\theta}{\gamma} z e^{-\gamma z}$	$M_{53}(z) = i\beta e^{\gamma z}$	$M_{54}(z) = i\beta e^{-\gamma z}$	$M_{55}(z) = -\alpha e^{\gamma z}$	$M_{56}(z) = -\alpha e^{-\gamma z}$
	$M_{61}(z) = \left(\frac{1+\theta}{\gamma} - \theta z \right) e^{\gamma z}$	$M_{62}(z) = - \left(\frac{1+\theta}{\gamma} + \theta z \right) e^{-\gamma z}$	$M_{63}(z) = \gamma e^{\gamma z}$	$M_{64}(z) = -\gamma e^{-\gamma z}$	$M_{65}(z) = 0$	$M_{66}(z) = 0$

$$\gamma = \sqrt{\alpha^2 + \beta^2}, \lambda = \nu E / (1 + \nu)(1 - 2\nu), G = E / 2(1 + \nu), \theta = (\lambda + G) / 2G = 1/2(1 - 2\nu)$$

Table II

$[A] =$	$M_{11}(z+)$	$M_{12}(z+)$	$M_{13}(z+)$	$M_{14}(z+)$	$M_{15}(z+)$	$M_{16}(z+)$	0						$c_1^{(+)}$	0
	$M_{21}(z+)$	$M_{22}(z+)$	$M_{23}(z+)$	$M_{24}(z+)$	$M_{25}(z+)$	$M_{26}(z+)$							$c_2^{(+)}$	0
	$M_{31}(z+)$	$M_{32}(z+)$	$M_{33}(z+)$	$M_{34}(z+)$	$M_{35}(z+)$	$M_{36}(z+)$							$c_3^{(+)}$	0
	$M_{11}(z_0)$	$M_{12}(z_0)$	$M_{13}(z_0)$	$M_{14}(z_0)$	$M_{15}(z_0)$	$M_{16}(z_0)$	$-M_{11}(z_0)$	$-M_{12}(z_0)$	$-M_{13}(z_0)$	$-M_{14}(z_0)$	$-M_{15}(z_0)$	$-M_{16}(z_0)$	$c_4^{(+)}$	$\Delta \Sigma_{zx}$
	$M_{21}(z_0)$	$M_{22}(z_0)$	$M_{23}(z_0)$	$M_{24}(z_0)$	$M_{25}(z_0)$	$M_{26}(z_0)$	$-M_{21}(z_0)$	$-M_{22}(z_0)$	$-M_{23}(z_0)$	$-M_{24}(z_0)$	$-M_{25}(z_0)$	$-M_{26}(z_0)$	$c_5^{(+)}$	$\Delta \Sigma_{zy}$
	$M_{31}(z_0)$	$M_{32}(z_0)$	$M_{33}(z_0)$	$M_{34}(z_0)$	$M_{35}(z_0)$	$M_{36}(z_0)$	$-M_{31}(z_0)$	$-M_{32}(z_0)$	$-M_{33}(z_0)$	$-M_{34}(z_0)$	$-M_{35}(z_0)$	$-M_{36}(z_0)$	$c_6^{(+)}$	$\Delta \Sigma_{zz}$
	$M_{41}(z_0)$	$M_{42}(z_0)$	$M_{43}(z_0)$	$M_{44}(z_0)$	$M_{45}(z_0)$	$M_{46}(z_0)$	$-M_{41}(z_0)$	$-M_{42}(z_0)$	$-M_{43}(z_0)$	$-M_{44}(z_0)$	$-M_{45}(z_0)$	$-M_{46}(z_0)$	$c_1^{(-)}$	ΔU
	$M_{51}(z_0)$	$M_{52}(z_0)$	$M_{53}(z_0)$	$M_{54}(z_0)$	$M_{55}(z_0)$	$M_{56}(z_0)$	$-M_{51}(z_0)$	$-M_{52}(z_0)$	$-M_{53}(z_0)$	$-M_{54}(z_0)$	$-M_{55}(z_0)$	$-M_{56}(z_0)$	$c_2^{(-)}$	ΔV
	$M_{61}(z_0)$	$M_{62}(z_0)$	$M_{63}(z_0)$	$M_{64}(z_0)$	$M_{65}(z_0)$	$M_{66}(z_0)$	$-M_{61}(z_0)$	$-M_{62}(z_0)$	$-M_{63}(z_0)$	$-M_{64}(z_0)$	$-M_{65}(z_0)$	$-M_{66}(z_0)$	$c_3^{(-)}$	ΔW
	0						$M_{41}(z-)$	$M_{42}(z-)$	$M_{43}(z-)$	$M_{44}(z-)$	$M_{45}(z-)$	$M_{46}(z-)$	$c_4^{(-)}$	0
0						$M_{51}(z-)$	$M_{52}(z-)$	$M_{53}(z-)$	$M_{54}(z-)$	$M_{55}(z-)$	$M_{56}(z-)$	$c_5^{(-)}$	0	
0						$M_{61}(z-)$	$M_{62}(z-)$	$M_{63}(z-)$	$M_{64}(z-)$	$M_{65}(z-)$	$M_{66}(z-)$	$c_6^{(-)}$	0	

The average value of q over R_j is given by

$$\bar{q}_j = \frac{1}{A_j} \int_{R_j} \int \mathbf{q} \, dA$$

so that from equation (9)

$$\begin{aligned} \bar{q} = & \int_{-\infty}^{\infty} \int_{-\infty}^{\infty} \Phi_j(\alpha, \beta) (D^{(-)} M(\alpha, \beta, z_0) N^{(-)}(\alpha, \beta) \\ & + D^{(+)} M(\alpha, \beta, z_0) N^{(+)}(\alpha, \beta)) \cdot \Delta \mathbf{P} \, d\alpha \, d\beta \end{aligned} \quad (10a)$$

where

$$\Phi_j(\alpha, \beta) = \frac{1}{A_j} \int_{R_j} \int e^{i(\alpha x + \beta y)} \, dA \quad (10b)$$

If it is assumed that, to sufficient accuracy, the dislocation can be considered to be constant over each sub-region R_k then it follows from equation (4b) that

$$\begin{aligned} \Delta \mathbf{P} = & \sum_{k=1}^n \frac{\Delta \mathbf{p}_k}{4\pi^2} \int \int_{R_k} e^{-i(\alpha x + \beta y)} \, dA \\ = & \sum_{k=1}^n \frac{A_k}{4\pi^2} \Phi_k^*(\alpha, \beta) \Delta \mathbf{p}_k \end{aligned} \quad (11)$$

where $\Phi_k^*(\alpha, \beta)$ is the complex conjugate of $\Phi_k(\alpha, \beta)$ defined by equation (10b) and A_k is the area of the sub-region R_k .

Substitution of equation (11) into equation (10) leads to the final form

$$\mathbf{q}_j = \sum_{k=1}^n I_{jk} \Delta \mathbf{p}_k$$

where

$$\begin{aligned} I_{jk} = & \int_{-\infty}^{\infty} \int_{-\infty}^{\infty} \frac{A_k}{4\pi^2} \Phi_j(\alpha, \beta) \Phi_k^*(\alpha, \beta) (D^{(-)} \cdot M(\alpha, \beta, z_0) \cdot N^{(-)}(\alpha, \beta) \\ & + D^{(+)} \cdot M(\alpha, \beta, z_0) \cdot N^{(+)}(\alpha, \beta)) \, d\alpha \, d\beta \end{aligned}$$

The evaluation of the term $\Phi_j(\alpha, \beta)$ is quite straightforward. For example, it can be easily shown for a rectangular sub-region R_j defined by the limits

$$|x - \bar{x}_j| \leq \frac{1}{2} \Delta x_j; \quad |y - \bar{y}_j| \leq \frac{1}{2} \Delta y_j$$

that

$$\Phi_j(\alpha, \beta) = \frac{4 \exp [i(\alpha \bar{x}_j + \beta \bar{y}_j)] \sin(\alpha \Delta x_j / 2) \sin(\beta \Delta y_j / 2)}{\Delta x_j \Delta y_j \alpha \beta}$$

Extension to a Fourier series representation

The analysis described in the previous section enables the calculation of the influence matrices I_{jk} for an isolated anchor. A case of some practical importance is that of a series of periodically spaced anchors with spacing $2W_x$ in the x direction and $2W_y$ in the y direction. In this case the solution is best represented as a Fourier series. Thus, typically the displacement in the x

HORIZONTALLY EMBEDDED ANCHORS

direction will have the representation:

$$u(x, y, z) = \sum_{-\infty}^{\infty} \sum_{-\infty}^{\infty} \exp [i(\alpha_n x + \beta_m y)] U(\alpha_n, \beta_m, z)$$

where

$$U(\alpha_n, \beta_m, z) = \frac{1}{4 W_x W_y} \int_{-W_y}^{W_y} \int_{-W_x}^{W_x} \exp [-i(\alpha_n x + \beta_m y)] u(x, y, z) dx dy$$

and

$$\begin{aligned} \alpha_n &= n\pi / W_x & n &= 0, \pm 1, \pm 2, \dots \\ \beta_m &= m\pi / W_y & m &= 0, \pm 1, \pm 2, \dots \end{aligned}$$

The analysis of this case parallels that described in the previous section, and it is found that for this case

$$\begin{aligned} I_{jk} &= \sum_{-\infty}^{\infty} \sum_{-\infty}^{\infty} \frac{A_k}{4 W_x W_y} \Phi_j(\alpha_n, \beta_m) \Phi_k^*(\alpha_n, \beta_m) \\ &\times [D^{(-)} \cdot M(\alpha_n, \beta_m, z_0) \cdot N^{(-)}(\alpha_n, \beta_m) + D^{(+)} \cdot M(\alpha_n, \beta_m, z_0) \cdot N^{(+)}(\alpha_n, \beta_m)] \quad (12) \end{aligned}$$

PREDICTION OF THE ELASTIC LOAD DEFLECTION BEHAVIOUR OF ANCHOR PLATES

The method of analysis presented in the previous section may be utilized to determine the stresses and displacements anywhere within the elastic soil mass due to a given load applied to an anchor of general shape. However, for the purpose of illustration, attention will be restricted here to the load displacement relationship for strip and circular anchors. A more detailed investigation, which includes consideration of rectangular anchors, has been presented by Rowe and Booker.⁶

The apparent stiffness of an isolated anchor depends primarily upon Poisson's ratio ν and three geometric parameters; namely, the anchor shape, the embedment ratio h/B , and the depth of the soil layer beneath the anchor D/B . Unless otherwise stated, the analysis has been performed for the basic case of a smooth rigid anchor resting in a soil underlain by a rough rigid base and with self-weight or applied surcharge sufficient to prevent breakaway of the anchor from the underlying soil, although the effect of certain secondary parameters has also been investigated.

Application of the analytical techniques described in the preceding section to the prediction of the load displacement behaviour of a rigid anchor involves a numerical approximation regarding the number of sub-regions which are necessary to simulate rigid anchor behaviour. In this regard it was found that the load-displacement relationship could be obtained to sufficient accuracy by sub-division of a strip into eight strip 'elements' and a circle into four annular rings. The adoption of a larger number of 'elements' did not significantly alter the apparent stiffness of the anchor. For example, in a strip analysis increasing the number of sub-regions ('elements') from eight to fourteen for a range of parameters (W/B , h/B , D/B and ν) increased the apparent stiffness by at most 0.8 per cent and generally by less than 0.4 per cent.

The analysis of anchor behaviour within a homogeneous elastic soil using this method of analysis only requires the solution of a small number of equations whereas alternative approaches which involve sub-division of the soil into numerous finite elements require the

solution of quite large systems of equations. Thus for an analysis of comparable accuracy, the proposed method of analysis leads to significant computational savings. Furthermore, these computational savings increase dramatically when considering deep anchors, deep soil layers and when considering the general three dimensional case of a rectangular anchor. A detailed investigation into the application of finite element techniques for the prediction of anchor behaviour up to and including collapse has been described by Rowe.⁷

The behaviour of strip anchors

Basic case. The effects of layer depth, embedment ratio and Poisson's ratio upon an isolated, rigid, strip anchor can be conveniently represented by expressing the apparent stiffness $P/\delta E$ in the form

$$\frac{P}{\delta E} = \frac{I_D(h/B = \infty) \cdot I_h}{(1 - \nu^2)} \quad (13)$$

where

- P is the applied load (per unit length) necessary to cause the anchor to displace a distance δ ,
- $I_D(h/B) = \infty$ is an influence factor for the effect of layer depth D/B upon the apparent stiffness evaluated for an anchor with $h/B = \infty$,
- I_h is a correction factor for the effect of embedment ratio h/B upon the apparent stiffness, and
- E and ν are Young's modulus and Poisson's ratio.

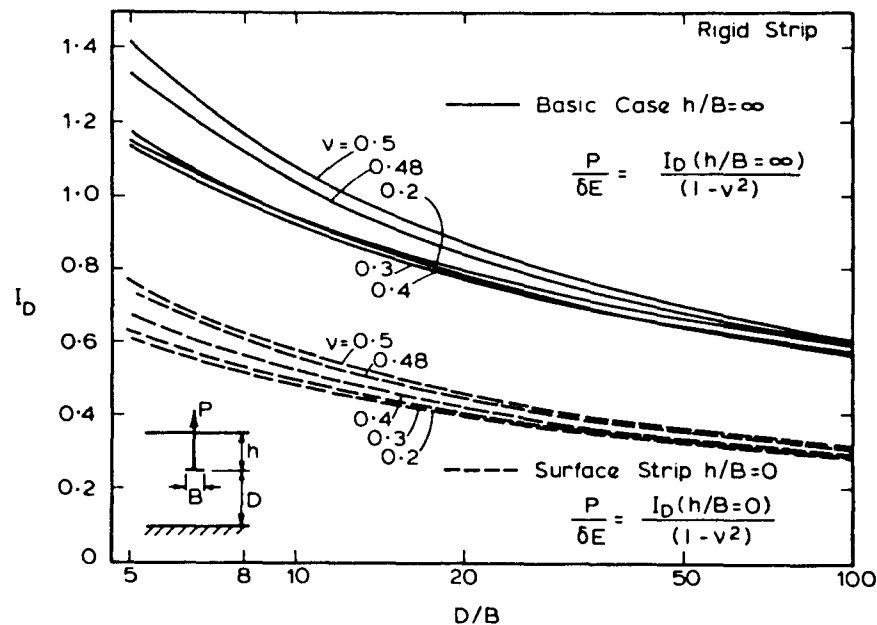


Figure 2. Influence factor I_D for the effect of layer depth upon elastic load deflection behaviour of a rigid strip

HORIZONTALLY EMBEDDED ANCHORS

The influence factor I_D is shown in Figure 2 as a function of layer depth D/B for the basic case of a rigid anchor with an infinite embedment ratio ($h/B = \infty$). For comparison purposes, the second limiting case of a rigid surface footing is also shown in this figure. It can be seen that the influence factor I_D is relatively insensitive to Poisson's ratio, varying by about 20 per cent at most, whereas the actual stiffness $P/\delta E$ varies by more than 50 per cent in the worst case. It will be observed that for the surface strip, the influence factor increases sensibly with Poisson's ratio; however, in the case of the anchor with an infinite embedment ratio there is no consistent trend for the curves with $\nu = 0.2, 0.3$ and 0.4 , although the maximum difference between these curves is less than 4 per cent. This behaviour is a manifestation of the removal of the factor $1/(1 - \nu^2)$ in determining I_D , and the actual stiffness itself does increase sensibly with Poisson's ratio. In view of the close bracketing of I_D with Poisson's ratio obtained by removing the factor $1/(1 - \nu^2)$, the disadvantage of having influence curves which intersect when plotted against D/B was not considered to be serious.

The correction factor I_h is shown in Figures 3(a), (b), (c) and (d) as a function of embedment ratio h/B for a range of layer depths D/B . This correction factor I_h corresponds to the ratio of the apparent stiffness for a given h/B to the apparent stiffness obtained for a similar case where $h/B = \infty$ and consequently, attains a value of unity at the limiting embedment ratio. Three observations can be made from Figure 3. Firstly, the limiting embedment ratio increases with layer depth. Secondly, the proportion of the maximum possible stiffness that can be obtained for a particular embedment ratio decreases dramatically with layer depth. Finally, it was found that the correction factor I_h is not particularly sensitive to the value of Poisson's ratio, varying by about 10 per cent, (over the range $0.2 \leq \nu \leq 0.5$) in the worst case.

The foregoing analyses were performed for the basic case of a fully bonded, smooth, rigid anchor resting in a layer underlain by a rough rigid base. The effect of varying these conditions upon the load deflection behaviour of the anchor will now be considered.

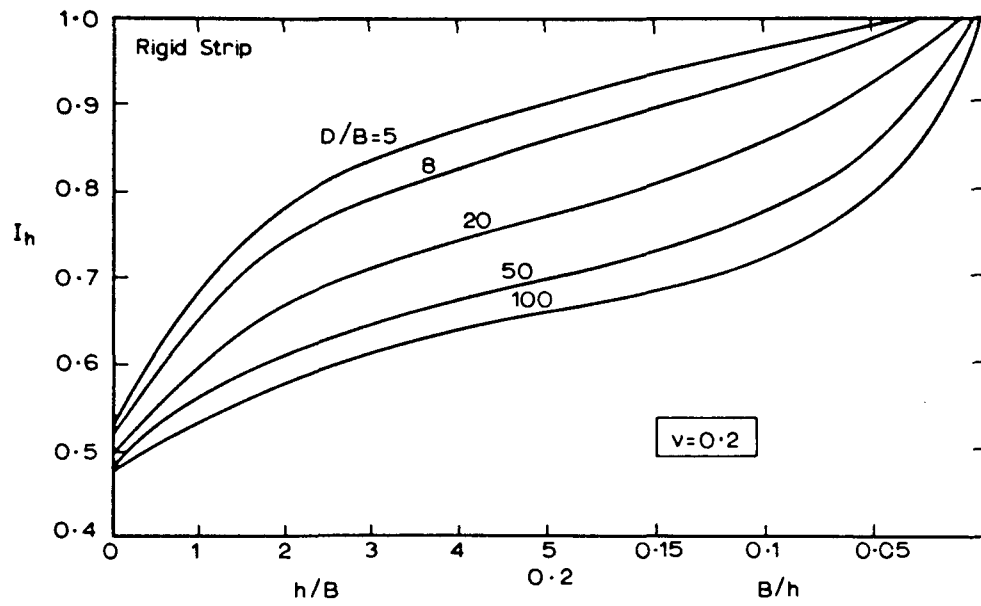
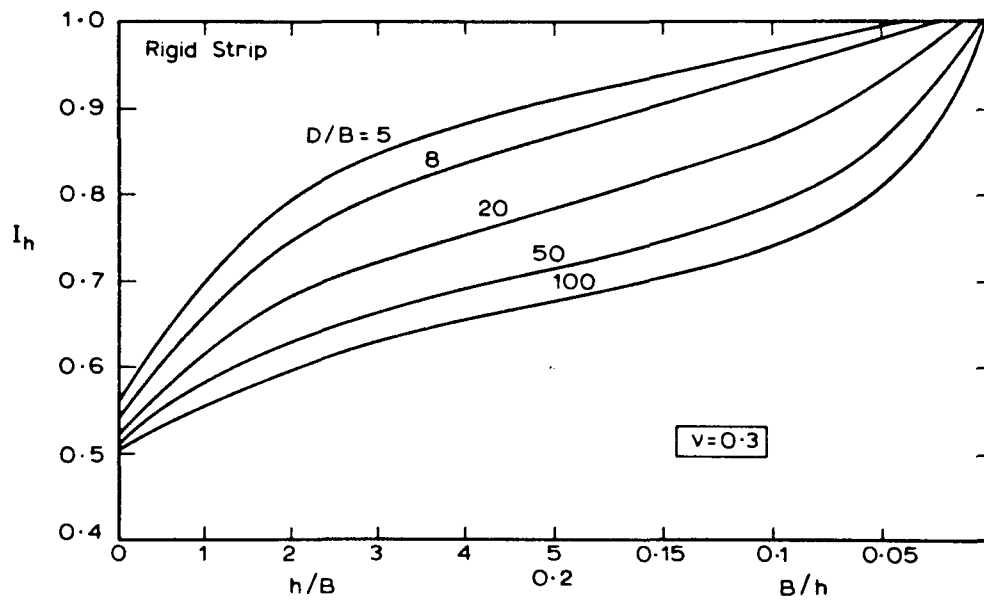
Effects of interface between soil layer and rigid base. To investigate the effect of the assumed boundary condition between the soil layer and the rigid base, analyses were performed for an anchor in a layer with $D/B = 8$ for the conditions of a rough and smooth rigid base. The apparent stiffnesses obtained from these analyses are shown in Figure 4. The smooth base condition was found to give stiffnesses which were about 4–6 per cent and 14–20 per cent lower than those obtained with a rough base for Poisson's ratio's of $\nu = 0.3$ and $\nu = 0.5$, respectively.

Since it might be expected that the effect of the base interface condition upon the apparent stiffness would decrease with layer depth D/B , analyses were also performed for an anchor at infinite depth ($h/B = \infty$), for a range of layer depths D/B using the two base conditions. The resulting stiffnesses are shown in Figure 5. From these results, it will be observed that although the significance of the base interface condition does decrease with layer depth D/B , the rate of decrease with depth is relatively slow.

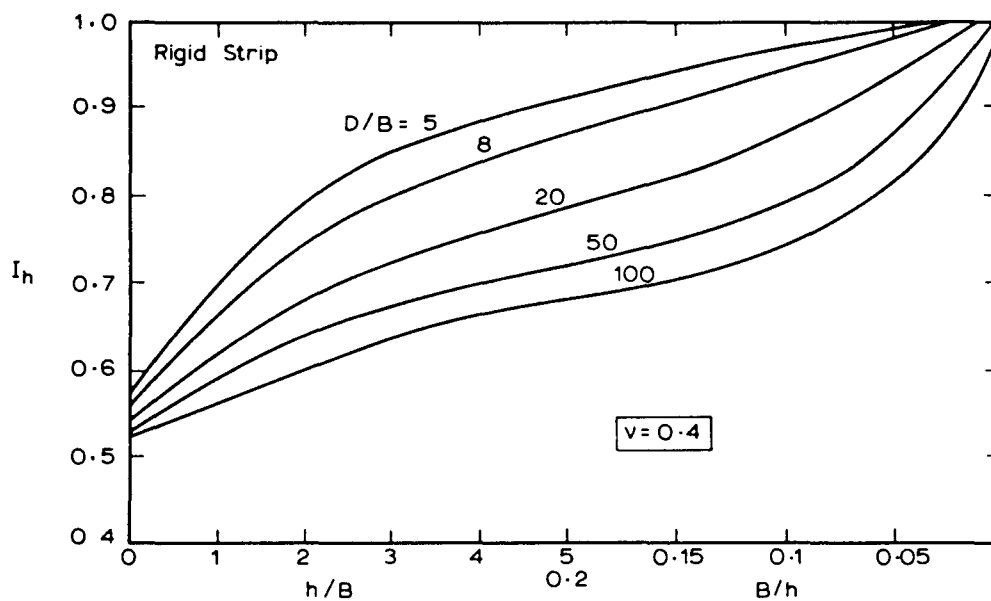
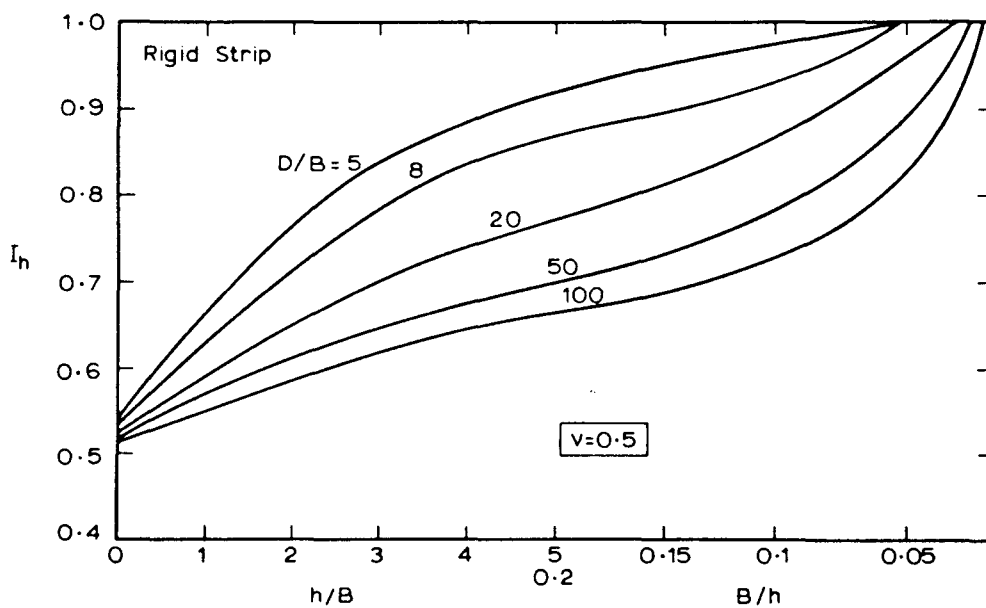
In general, it is considered that the rough base condition would be the more practical case; however, if the type of base is considered to be significant, then the predicted stiffness obtained for a rough base using equation (13) can be approximately modified for a smooth base by multiplying this stiffness by the ratio of smooth to rough stiffness obtained for the particular layer depth D/B from Figure 5.

Effect and anchor roughness. The type of interface condition between the anchor and soil was found to be unimportant in the determination of the apparent stiffness, since the difference between the stiffnesses obtained for smooth and rough anchors was always less than 1 per cent and often less than 0.1 per cent for a wide range of layer depths, embedment ratios and values of Poisson's ratio.

R. K. ROWE AND J. R. BOOKER

Figure 3(a). Correction factor I_h for the effect of embedment ratio— $\nu = 0.2$ Figure 3(b). Correction factor I_h for the effect of embedment ratio— $\nu = 0.3$

HORIZONTALLY EMBEDDED ANCHORS

Figure 3(c). Correction factor I_h for the effect of embedment ratio— $\nu = 0.4$ Figure 3(d). Correction factor I_h for the effect of embedment ratio— $\nu = 0.5$

R. K. ROWE AND J. R. BOOKER

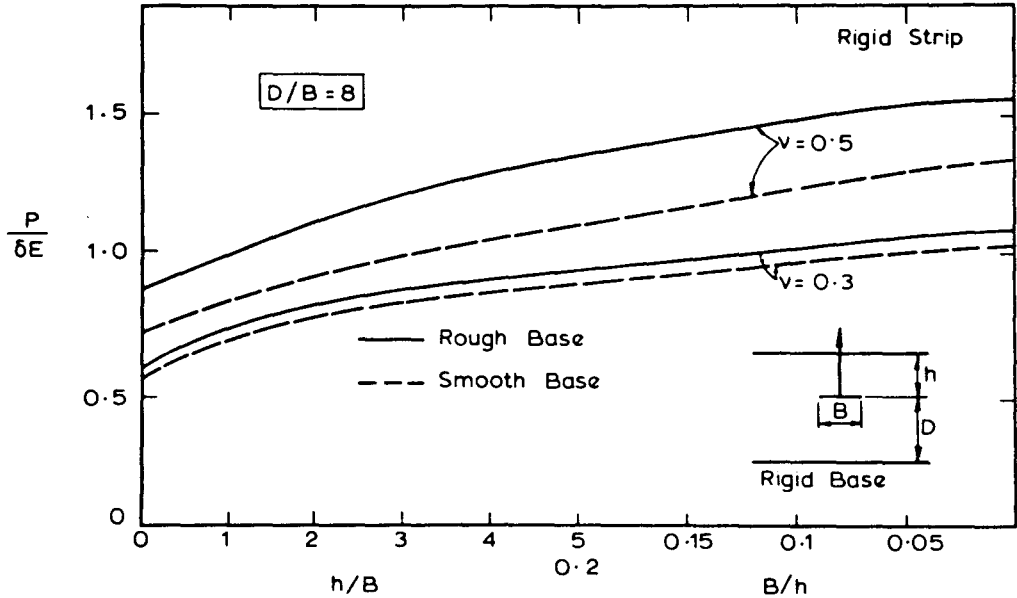


Figure 4. Effect of base condition upon apparent stiffness

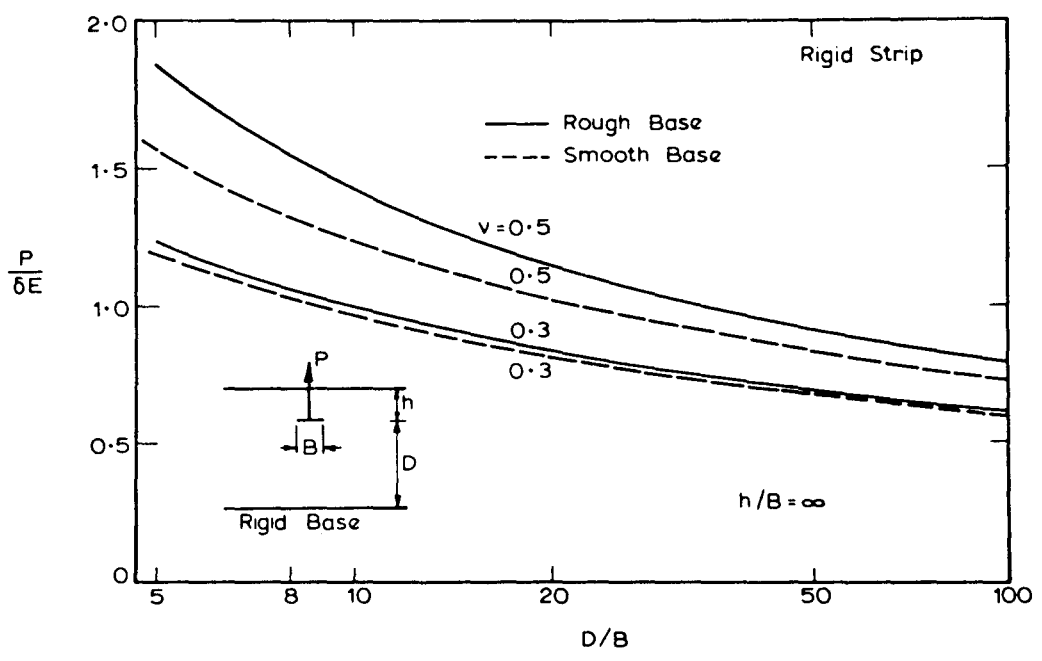


Figure 5. Effect of base condition upon apparent stiffness

HORIZONTALLY EMBEDDED ANCHORS

Effect of anchor rigidity upon apparent stiffness. The apparent stiffness calculated on the basis of the mean displacement of a uniformly loaded region (corresponding to an infinitely flexible anchor) was found to differ from the stiffness determined for a rigid anchor by between 3 and 6 per cent for a wide range of geometric parameters and value of Poisson's ratio. Thus it can be concluded that, provided the loading arrangement does not cause structural failure of the anchor plate itself or alter its geometry significantly, the flexibility of the anchor will not greatly alter the load-(mean) deflection behaviour of the anchor.

Effect of breakaway. It is generally accepted (e.g., Douglas and Davis⁸, Selvadurai²) that the fully bonded (no breakaway) condition corresponds to the most practical limiting case for the application of elastic solutions, since at working loads the compressive stresses due to overburden pressure will usually be sufficiently large to prevent the development of tensile stresses between anchor and soil. Accordingly, the majority of solutions presented in this paper are for the case of a fully bonded anchor; however, as outlined in the second section, analyses can be performed for the case where there is breakaway of the anchor from the soil. Assuming that there is no adhesion or suction acting between the anchor plate and the soil, then breakaway will occur when the vertical stress below the anchor is zero. Breakaway corresponds to a separation of anchor from the underlying soil and results in the formation of a gap below the anchor. Immediate breakaway occurs when the vertical stress below the anchor is initially zero, and consequently any increment in load will result in complete separation of the anchor from the underlying soil. To illustrate this effect, the apparent stiffnesses obtained when there is immediate breakaway are shown in Figure 6 for an anchor resting in a layer with depth ratio

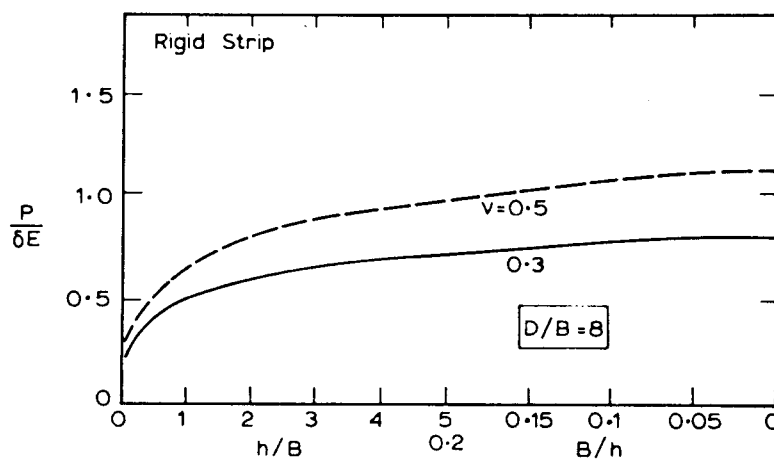


Figure 6. Effect of immediate breakaway upon apparent stiffness

$D/B = 8$. Comparison of the apparent stiffnesses obtained for the two cases of immediate breakaway and no breakaway (i.e., Figures 4 and 6) indicates that the influence of breakaway decreases with increasing embedment ratio, while it increases with Poisson's ratio.

The situation in which there is progressive breakaway with increasing load can also be analysed by adopting an incremental procedure (Rowe and Booker⁶).

Effect of interaction between anchors with an infinite group. By replacing the Fourier integral representation (equation (4)) by a Fourier series expansion (e.g., see equation (12)), it is possible

